

Synthesis and nano structural study on $\text{TiO}_2\text{-NiO-SiO}_2$ composite

ABSTRACT

M. Riazian*

*Department of Engineering,
Tonekabon branch, Islamic Azad
University, Tonekabon, Iran.*

Received: 09 December 2012

Accepted: 15 March 2013

We report on the synthesis, morphology, chemically and structurally of $\text{TiO}_2\text{-NiO-SiO}_2$ nanostructure. The $\text{TiO}_2\text{-NiO-SiO}_2$ nanostructure was synthesized by a method based on the sol-gel method, by the simultaneous gelation of all cations. The coatings were deposited on dried soda-lime glass slides by spin coating. Composite powders and coating on glass have been characterized by XRD, SEM, EDAX, and FTIR. X-ray diffraction showed the formation of nano crystalline, anatase, TiO_2 , NiO and NiTiO_3 phases. Scanning electron microscopy revealed that nanostructure formed by increasing the calcinations temperatures. EDX spectroscopy confirmed the composition of the ternary powders and coating, which were formed during the gelation process. The effects of chemical compositions and calcinations temperature on the surface topography and the crystallization of phases were studied. The activation energy (E) of nanoparticles formation during thermal treatment was calculated.

Keywords: Nanostructure; Poly-component; $\text{TiO}_2\text{-NiO-SiO}_2$; Activation energy; Sol-Gel method.

INTRODUCTION

Titania is known to have three natural polymorphs, i.e. rutile, anatase, and brookite. Only anatase (Figure 1) is generally accepted to have significant activity. Titanium dioxide (TiO_2) is well known as a photocatalyst and widely applied for air and waste water purification. The performance of these compounds depends on the characteristic of the TiO_2 crystallites, such as the size and surface area. Therefore, modification of its physical and chemical property is of interest to researchers. One of the possible ways to modify the property of TiO_2 crystallites is by adding a second semiconductor into the TiO_2 matrix. SiO_2 has high thermal stability, excellent mechanical strength and help to create new catalytic sites due to interaction between TiO_2 and SiO_2 [1] also, SiO_2 acts as a carrier of TiO_2 and helps to obtain a large surface area as well as a suitable porous structure [2].

* Corresponding author:

M. Riazian
Department of Engineering,
Tonekabon branch, Islamic Azad
University, Tonekabon, Iran.
Tel +98 9122116905
Fax +98 1924274409
Email m.riazian@toniau.ac.ir

Archive of SID

Recently, many researchers demonstrate that mixed metal oxide enhance the structural performance due to improved surface adsorption and increasing surface hydroxyl group. During the last years many studies dealing with TiO_2 doping with different metals have shown the alterations that the dopant may cause on the catalyst surface [3–6].

NiO nano sized particles have attracted much attention as it has been used in magnetic devices, fuel cell electrodes, gas sensors, photovoltaic devices and electrochromic films [7–9]. Nanoparticles or nanostructures such as NiO act as catalysts for growing CNT.

Titania can be synthesized by various techniques, such as precipitation [11], chemical vapor deposition [12], hydrothermal method [13] and glycothermal method [14]. Another common technique that can result titania with extremely high surface area is sol-gel method. The sol-gel process is one of the versatile methods to prepare ceramic materials. Currently, the sol-gel process is employed quite often for synthesis of nano-size catalytic materials. The incorporation of an active metal in the sol during the gelation stage allows the metal to have a direct interaction with support, therefore the material possess special catalytic properties. The design of advanced ceramics depends on the availability of powders with outstanding properties in terms of composition, purity, size, and size distribution. Sol-gel processes allow synthesis powders to have a more elaborate structure. The synthesis of inorganic materials such as metal oxides with different morphologies for specific applications has attracted a considerable amount on interest in recent years, and has been a challenging issue for chemists and material researchers. It is well recognized that the properties of materials highly depend on size, morphology, and dimensionality [15], three crucial geometric parameters. The sol-gel process is commonly applied to synthesis such TiO_2 materials owing to its several advantages such as low temperature processing and the ability to prepare materials in various shapes, compared with the conventional preparation procedures of glass and ceramics. [16, 17].

Among all metal oxides, TiO_2 powders and coatings are extensively used as catalysts, adsorbents, composites, ceramics, and catalyst supports because of their high surface area and

significant pore volume. In this work we prepare TiO_2 -NiO- SiO_2 by using hydrolysis procedure of tetra isopropyl ortho titanate and nickel nitrate which is transformed to anatase, TiO , NiO and NiTiO_3 by heating it at 300, 600, 750 and 950 °C. The structure obviously depends on the preparation procedures and TiO_2 content in combination.



Fig. 1. Schematic model of anatase.

EXPERIMENTAL

The composition of the starting solution and the experimental conditions used for ternary powders are listed in Table 1. Figure 2 illustrates the preparation procedures. The precursors: tetraethoxysilane (TEOS, Merk, $\geq 99\%$), titanium tetra isopropoxide ($\text{Ti}(\text{OPri})_4$, Merk $\geq 98\%$), $(\text{Ni}(\text{NO}_3)_2 \cdot 6\text{H}_2\text{O}$ Applichem, $\geq 99\%$), HCl (Merk, 36%), Ethanol (Merk $\geq 99\%$) and deionized water were used without further purification.

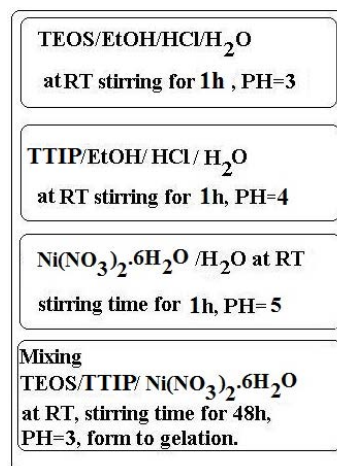


Fig. 2. Schematic flow chart illustrating the steps in the synthesis pathway of TiO_2 -NiO- SiO_2 nanomaterials.

Archive of SID

The starting point for the synthesis was a solution prepared by mixing precursors: (TEOS, deionized water, ethanol, HCl), (TTIP, deionized water, ethanol, HCl) separately at room temperature (RT) for 1 hour. Nickel nitrate was added to the result solution according to molar ratio in Table 1. After then, above solutions mixed vigorously at RT. Gelation was formed after 48 h stirring. Afterward, the gel was dried for about 24 h at 50 °C temperature in air and calcined at 10°C/min to four different temperatures (300, 600, 750 and 950 °C) and held there for 2 h. Moreover, the effects of varied calcinations temperature were studied with as-prepared, 300, 600, 750 and 950 °C. The coating was deposited on dried soda-lime glass slides by spin coating. The coatings after dried in air were heated at 10 °C/min to 300 °C and held there for 2h.

Characterization of the TiO_2 -NiO- SiO_2

- **X-ray powder diffraction study**

X-ray powder diffraction (XRD) patterns were measured on a (GBC-MMA 007 (2000)) X-ray diffractometer. The diffractograms were recorded with (K_α (Cu), 1.54 Å, 0.02° step size in where the speed was 10 $\frac{deg}{min}$) radiation over a 2θ range of 10°–80°.

- **Scanning electron microscopy**

SEM (XL30 Philips) was routinely used to investigate the morphology of the nanoparticles. Further investigation was confirmed with EDX to determine the chemical composition in the sample.

- **FT-IR study**

FT-IR measurements were performed on a 1730 Infrared Fourier Transform Spectrometer (Perkin-Elmer) using the potassium bromide as the background.

RESULTS AND DISCUSSION

Figure 3 and assignments of the XRD peaks are summarized in Table 2. Due to different calcined temperatures, crystalline phases are formed. Figure 3 shows the XRD patterns of powder obtained from gels after drying and calcinating at 300 °C, 600 °C, 750 and 950 °C with 10 $\frac{C^\circ}{min}$ gradient and stayed in 2 hours, after then, they cooled in similar temperature gradient. This figure shows the amorphous structure for as-prepared, sample due to the short range ordering of the network [18]. Figures 1 and 3, also show anatase phase. Anatase phase is tetragonal with crystalline system ($a=3.7850 \text{ Å}$, $c=9.5140 \text{ Å}$). Sample obtained from 950 °C have a high degree of the crystallinity and show anatase, TiO_2 , NiO and $NiTiO_3$ phases. The grain size values were calculated from Scherrer equation:

$$r = \frac{k\lambda}{2\beta \cos \theta}$$

Where β was FWHM observed, shape factor k was assumed to be 0.9 and λ was a wavelength of CuK α radiation (0.154056 nm).

Table 1. Composition of starting solutions and experimental conditions for ternary powders preparation.

Method used	Method step	Precursor	Molar ratio (MR) TEOS/ TTIP/Ni(NO ₃) ₂ .6H ₂ O=1:1/0.5	Stirring Time(h)	pH
Alkoxide route	1	TEOS	TEOS/EtOH/HCl/H ₂ O=1:50/0.1/2	1	3
		TTIP	TTIP/EtOH/HCl/H ₂ O=1:50/0.1/2		4
		Ni(NO ₃) ₂ .6H ₂ O	Ni(NO ₃) ₂ .6H ₂ O /H ₂ O =1:0.02		5
	2	Mixing the precursors		1	3

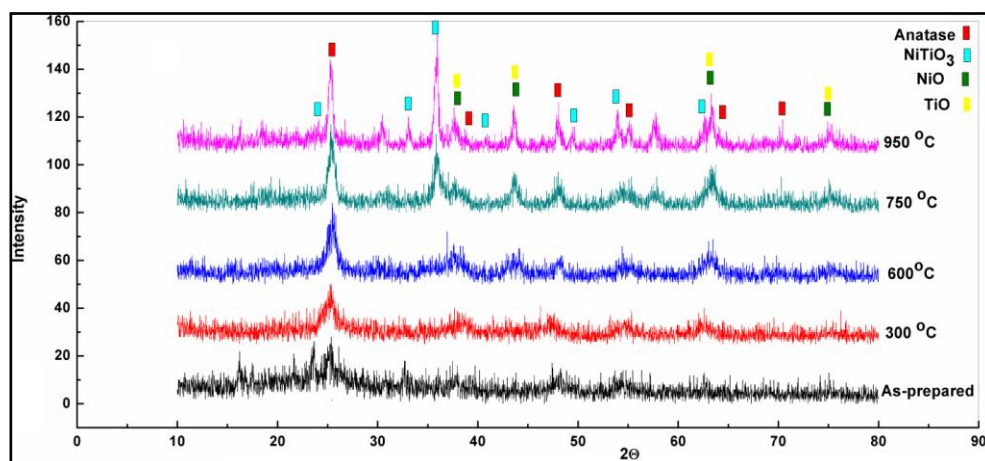


Fig. 3. XRD patterns of $\text{TiO}_2\text{-NiO-SiO}_2$ obtained from: without hydrothermal treatment (as-prepared), calcined at 300 °C, calcined at 600 °C, calcined at 750 °C, and calcined at 950 °C.

Table 2. The 2θ angle, d-space, Miller indexes, grain size of $\text{TiO}_2\text{-NiO-SiO}_2$.

Pure state															
Crystalline Phase	As-prepared			Calcined at 300 °C			Calcined at 600 °C			Calcined at 750 °C			Calcined at 950 °C		
	2Θ	d-space	size	2Θ	d-space	size	2Θ	d-space	size	2Θ	d-space	size	2Θ	d-space	size
	(Å) nm			(Å) nm			(Å) nm			(Å° nm			(Å°) nm		
Anatase Tetragonal a=3.8040 Å c=9.6140 Å	25.36	3.50	9	25.38	3.50	11	25.50	3.49	16	25.34	3.50	19	25.20	3.51	20
TiO Cubic a=4.1766 Å	-----			-----			37.60	2.38	53	37.50	2.38	60	33.35	2.69	70
NiO Cubic a=4.1684 Å	-----			-----			43.50	2.07	30	43.64	2.07	35	43.58	2.07	58
NiTiO ₃ Rhombohedral a=5.4500 Å c=13.2700 Å	-----			-----			-----			35.82	2.50	25	35.96	2.48	41

Since the atomic radii of Si atom is smaller than Ti, the TiO_2 particle experiences a contraction and its crystalline growth is retarded due to the Si atom. However, high composition of SiO_2 component leads to the formation of larger second particles of TiO_2 . This is due to the SiO_2 which behaves as a “neck” and connects the TiO_2 particles [19,20]. Data in Table 2 shows the influence of hydrothermal treatment (calcination) on the grain size of anatase and other phases.

The average crystal sizes of the nanopowders in pure state were calculated based on

the Scherrer's formula. Figure 4 shows the variation of XRD crystal size (D) of nanoparticles prepared by the thermal treatment of nanopowders at different temperatures. It can be indicated that the crystal size of NiO increased rapidly from about 35nm at 750 °C to 58nm at 950 °C, while crystal size of anatase increased correspondingly slowly. This is directly related to the crystallization of nanoparticles. Straight lines of $\ln D$ against $1/T$ (Figure 5) are plotted according to the Scott [21] equation given below under the condition of homogeneous growth of nanocrystallites, which

Archive of SID

approximately describes the crystal growth during annealing:

$D = C \exp(-E/RT)$ where C is a constant, E is the activation energy, R is the gas constant, and T is the absolute temperature. There exists a good linear relationship. The E value was calculated from the slope of the straight line as $E = 2.62$ kJ/mol for anatase, 6.79 kJ/mol for TiO and 16.52 kJ/mol for NiO. It shows that the calcination temperature has a more remarkable effect on the growth of nanocrystallites.

SEM images of $\text{TiO}_2\text{-NiO-SiO}_2$ nanoparticles are shown as Figures (6 and 7). As shown in Figure 7, it is obvious that larger particle size is achieved by increasing the calcinations process and this is consistent with XRD results. It can be indicated that the particle size in as-prepared state is 28 nm, in 300°C is 34 , in 600°C is 45 nm, in 750°C is 58 nm and in 950°C is 53 nm. Figure 6 showed partly uniform cover on the coating surface. The nanoparticles formed in the interfacial of fractures.

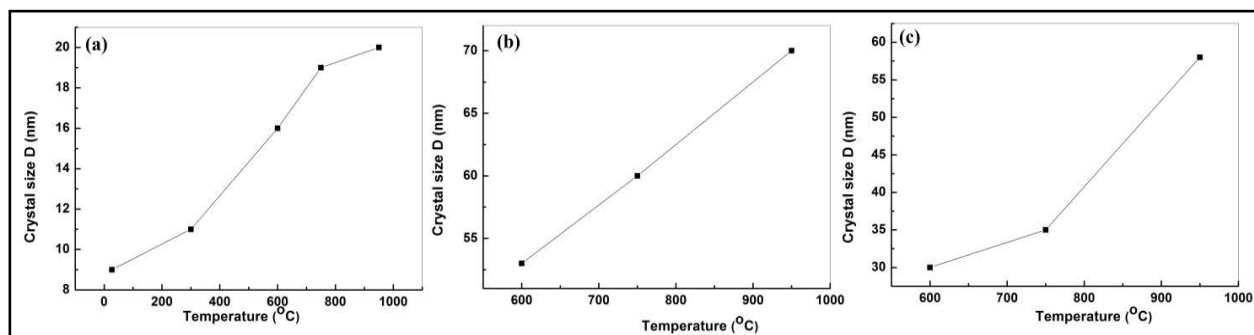


Fig. 4. Effect of thermal treatment temperature on particle size of (a) anatase (b) TiO (c) NiO.

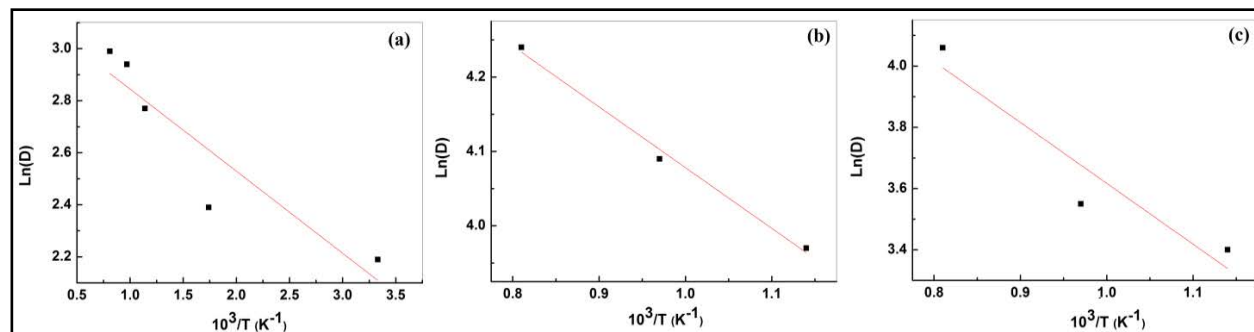


Fig. 5. Plot of $\ln D$ as a function of calcination temperature for the (a) anatase (b) TiO (c) NiO.

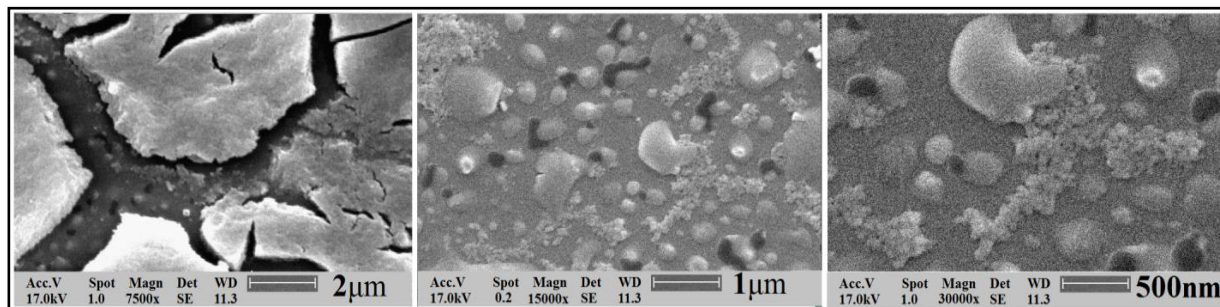


Fig. 6. SEM images of $\text{TiO}_2\text{-NiO-SiO}_2$ coating on glass calcined at 300°C .

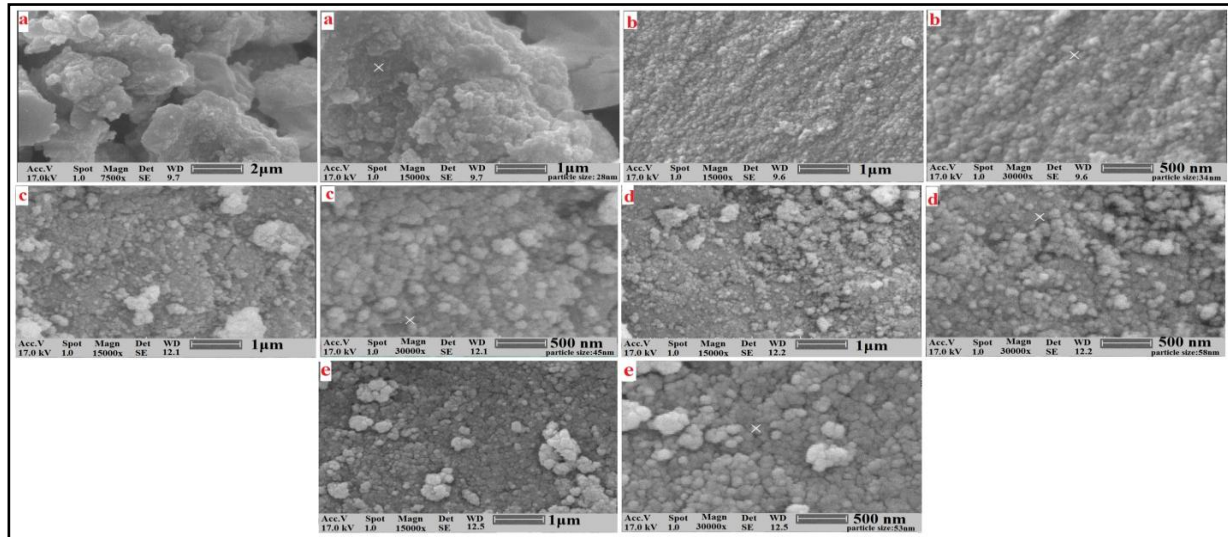


Fig. 7. SEM images of powder samples a) as-prepared and calcined at: b) 300 °C, c) 600 °C, d) 750 °C, e) 950 °C.

As can be seen in Figure 8 and Table 3, EDX spectra showed the element and atomic percent of materials for powder and coating

samples according to Figures 6 and 7. The results indicated the presence of TiO_2 , NiO and SiO_2 in the powder and coating samples.

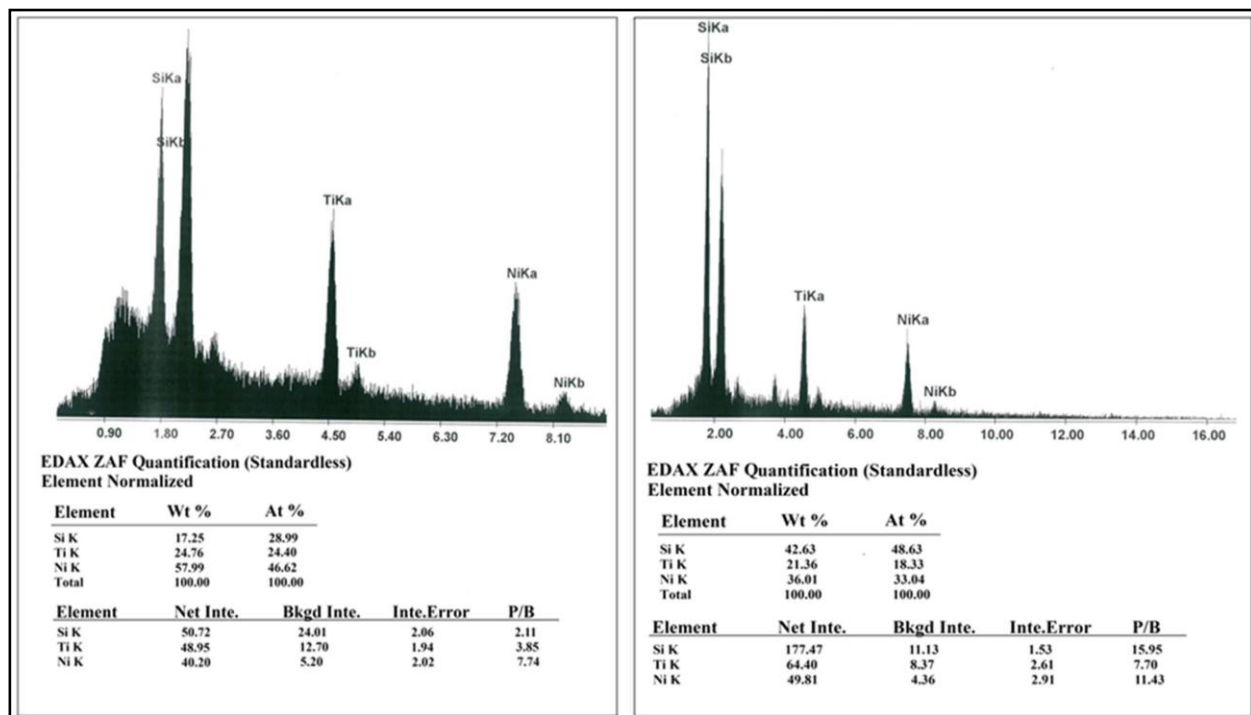
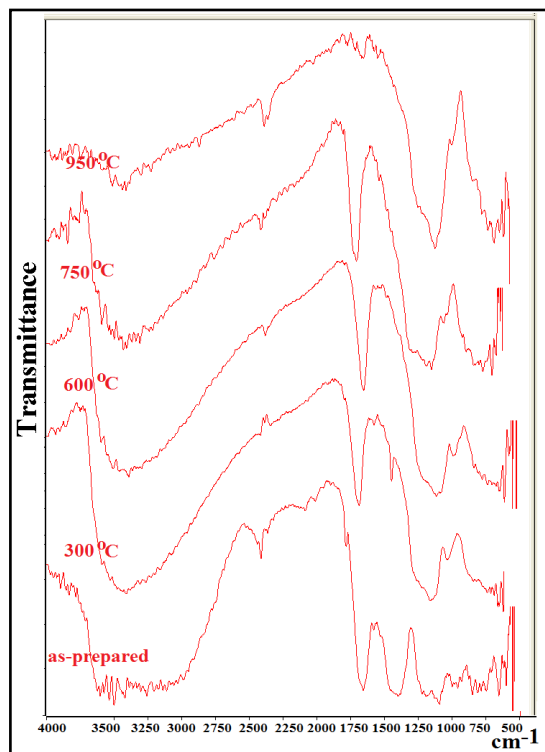


Fig. 8. EDX results for powder composite left) elementary analysis for powder and right) elementary analysis for coating sample.

Table 3. Chemical composition obtained from EDX.

Powder sample			
Element	Weight percent	Atomic percent	Error(%)
Si	17.25	28.99	2.06
Ti	24.76	24.40	1.94
Ni	57.99	46.62	2.02
Coating sample			
Si	42.63	48.63	1.53
Ti	21.36	18.33	2.61
Ni	36.01	33.04	2.91

The FTIR spectra of different calcinations temperature of powder were recorded in the wave number range of 400-4000 cm^{-1} (Figure 9).

**Fig. 9.** FTIR spectra of $\text{TiO}_2\text{-NiO-SiO}_2$ composite calcined at different temperature.

The polytitanosiloxane-composite of each sample shows the fundamental vibration modes. In the prepared gel, the 3200 cm^{-1} band has to be

attributed to hydroxyl groups (Ti-OH) and to OH from water and ethanol, which are occluded in the titania pore. The OH bending band of water in the gel is observed at 1650 cm^{-1} and the low energy interval the Ti-O band are found at 1061 cm^{-1} and 960 cm^{-1} . The IR spectra show peaks characteristic of Si-O (1050 cm^{-1}), Si-O-Ti (925 cm^{-1}), Ti-O (653–540 cm^{-1}) and Ti-O-Ti (495–436 cm^{-1}). When the composite was calcined at 950 $^{\circ}\text{C}$, the high-energy stretching band almost fades and the 1600 and 3225 cm^{-1} bending vibration band intensity decreases due to vaporization of the liquid. Nitrate groups are identified by the bands in the range of 1240-1480 cm^{-1} , by increasing the calcination temperature, the intensity of this band decreased due to vaporization of nitrates. It was being mentioned that the Ni-O stretching vibration at 460 cm^{-1} is hindered by the stronger rocking mode of the SiO_2 [22].

CONCLUSIONS

The homogeneous hydrolysis of metal alkoxide provided an excellent technique to prepare nanoparticle material. Experimental results indicated that the homogeneous hydrolysis of titanium tetra isopropoxide and nickel nitrate via sol-gel route is a promising technique for preparing material with uniform nanoparticles. In this study, nanocrystalline $\text{TiO}_2\text{-NiO-SiO}_2$ particles have been successfully synthesized by chemical method and heat treatment process. Samples calcined at different temperature and average crystallite sizes increased with an increase in calcined temperatures.

The effect of $\text{TiO}_2\text{-NiO-SiO}_2$ composite on the structural properties of powder and coating prepared by sol-gel (spin coating) technique has been examined. The powders calcined at 300, 600, 750 and 950 $^{\circ}\text{C}$. The coating sample calcined at 300 $^{\circ}\text{C}$. X-ray diffraction spectra showed anatase, TiO, NiO and NiTiO_3 phases and grains size. The activation energy of nanoparticles were calculated, $E=2.62$ kJ/mol for anatase, 6.79 kJ/mol for TiO and 16.52 kJ/mol for NiO. Scanning electron microscopy measurements showed nanostructure and morphology of powders and films. Chemical composition of samples was determined by EDX. The activation energy for mentioned nanocrystallite growth during

Archive of SID

calcinations was calculated. FTIR spectra of the ternary composite was presented and showed the possible bonds (Si-O, Ti-O and Ti-O-Si) and the Ni-O stretching vibration at 460 cm⁻¹ is hindered by the stronger rocking mode of the SiO₂.

ACKNOWLEDGEMENTS

The authors thank Islamic Azad University, Tonekabon branch for financial support through a research project.

REFERENCES

- [1] Ennaoui A., Sankapal B. R., Skryshevsky V. and lux-Stiener M. C., (2006), TiO₂ and TiO₂-SiO₂ thin films and powders by one-step soft-solution method: Synthesis and characterizations, *Sol Energy Matter. Sol cells*, 90: 1533-1541.
- [2] Shen M., Wu Z., Huang H., Du Y., Zou Z. and Yang P., (2006), Carbon-doped anatase TiO₂ obtained from TiC for photocatalysis under visible light irradiation. *Mat. Lett.* 60(5): 693-697
- [3] Jeon M. S., Yoon W. S., Joo H., Lee T. K. and Lee H., (2000), Preparation and characterization of a nano-sized Mor Ti mixed photocatalyst *Appl. Surf. Sci.* 165: 209-216.
- [4] Gesenhues V. and Photochem J., (2001), Al-doped TiO₂ pigments: influence of doping on the photocatalytic degradation of alkyd resins, *Photobiol. A: Chem.* 139: 243-251.
- [5] Riazian M. and Bahari A., (2012), Synthesis and Nanostructural Investigation of Doped TiO₂ Nanorods by SiO₂ Pramana *J. of Phys.* 78:319-331.
- [6] Riazian M. and Bahari A., (2011), The Growth of Thin TiO₂ Film and Nano Size TiO₂ Powder, *Int. J. of the Physical Sciences*, 6: 3756-3767.
- [7] Vaidya S., Ramanujachary K. V., Lofland S. E. and Ganguli A. K., (2009), Synthesis of Homogeneous NiO-SiO₂ Core-shell Nanostructures and the Effect of Shell Thickness on the Magnetic Properties *Cryst Growth Des*, 9: 1666-1670.
- [8] Ahmad T., Ramanujachary K. V., Lofland S. E., Ganguli A. K., (2006), Magnetic and electrochemical properties of nickel oxide nanoparticles obtained by the reverse – micellar route *Solid State Sci*, 8: 425–430.
- [9] Huang X. H., Tu J. P., Chen X. T., Yuan Y. F., Wu H. M., (2007), Spherical NiO-C composite for anode material of lithium ion batteries, *Electrochim Acta*, 52: 4177–81.
- [10] Huang J. H., Lin N. H., Chuang C. C., Lai H. W. and Hsu J. H., (2005), Selective growth of carbon nanotubes on nickel oxide templates created by atomic force microscope nano-oxidation *Diamond and Related Materials* 14: 744-748.
- [11] Kim S. J., Park S. D., Jeong Y. H. and Park S., (1999), Homogeneous precipitation of TiO₂ ultrafine powders from aqueous TiOCl₂ solution, *J. of the American Ceramic Soc.*, 82 , 927–932.
- [12] Ding Z., Hu X. J., Lu G. Q., Yue P. L., Greenfield P. F., (2000), Novel silica gelsupported TiO₂ photocatalyst synthesized by CVD method, *Langmuir*, 16 , 6216–6222.
- [13] Yang J., Mei S., Ferreira J. M. F., (2000), Hydrothermal synthesis of nanosized titania powders: influence of tetraalkyl ammonium hydroxides on particle characteristics, *J. of the American Ceramic Soc.*, 8: 1696–1702.
- [14] Iwamoto S., Tanakulrungsank W., Inoue M., Kagawa K. and Praserttham P., (2001), Synthesis of large-surface area silica-modified titania ultrafine particles by the glycothermal method, *J. of Mater.Sci.Let.*, 19 , 1439–1443.
- [15] Riazian M. Bahari A., (2012), Structure, Effect of Lattice Strain and Effect of sol

Archive of SID

Concentration on the Characterization of TiO₂-CuO-SiO₂ Nanoparticles, *Int. J. of Nano Dimensions*, 28: 127-139.

- [16] R. W. Scott R. W., M. J. Maclachlan M. J., Ozin G. A. and Curr O., (2003), Synthesis of Metal Sulfide Materials with Controlled Architecture *Solid State Mater Sci*, 4:113–121.
- [17] Li M., Lebeau B. and Mann S., (2003), Synthesis of aragonite nanofilament networks by mesoscale self-assembly and transformation in reverse microemulsions *Adv Mater* 15: ,2032–2035.
- [18] Y. Yin, A. P. Alivisatos, *Nature*, 437, 664–70 (2005).
- [19] Kato K., Tsuzuki A., Taoda H., Torii Y., Kato T. and Butsugan Y., (1994), Crystal Structures of TiO₂ Thin Coatings Prepared from the Alkoxide Solution via the Dip-Coating Technique Affecting the Photocatalytic Decomposition of Aqueous Acetic Acid, *J. Mater. Sci*, 29: 5911–15.
- [20] Abe Y., Sugimoto N., Nagao Y. and Misono T., (1988), Preparation of Monolithic SiO₂-TiO₂ Gels by Condensation Polymerization of Silicic Acid and Titanium Chelates, *J. Non-Cryst. Solids*, 104:164–69.
- [21] Scott M. G., (1983), Amorphous Metallic Alloys, Butterworth, *London*, pp.151.
- [22] Hernandez-Torres J. and Mendoza A., (2005), Formation of NiO-SiO₂ nanocomposite thin films by the sol-gel method, *J. of Non-Crys. Solids*, 351: 2029-2035.

Cite this article as: M. Riazian: Synthesis and nano structural study on TiO₂-NiO-SiO₂ composite.
Int. J. Nano Dimens. 5(2): 123-131, Spring 2014